Bull. Inst. Chem. Res., Kyoto Univ., Vol. 72, No. 2, 1994

Optical Properties of Transparent Glass-Ceramics Containing $ZnGa_2O_4:Cr^{3+}$ Microcrystals

Katsuhisa TANAKA*, Iwao YAMAGUCHI*,
Kazuyuki HIRAO* and Naohiro SOGA*

Received May 25, 1994

Transparent glass-ceramics containing $ZnGa_2O_4:Cr^{3+}$ have been prepared by the heat treatment of glass in sodium zinc gallate silicate system for the purpose of evaluating optical properties of the $ZnGa_2O_4:Cr^{3+}$ microcrystal precipitated in the glass matrix. Average crystallite size of the $ZnGa_2O_4:Cr^{3+}$ microcrystal estimated from the full width at half maximum of X-ray diffraction peak is about 100 A. The optical absorption spectra indicate that the ligand field strength around the Cr^{3+} ion is higher in the $ZnGa_2O_4:Cr^{3+}$ microcrystal than in the glass, which is coincident with the fact that the *R*-line is observed in the emission spectrum of the transparent glass-ceramics while the emission spectrum of glass manifests a broad Stokes' shifted band. We have analyzed temperature dependence of peak position of R_1- and R_2-lines for the $ZnGa_2O_4:Cr^{3+}$ microcrystal and polycrystal by assuming the Raman process for the electronic transition and the Debye model for the vibrational density of state. The Debye temperatures of $ZnGa_2O_4:Cr^{3+}$ microcrystal estimated from the R_1- and R_2-lines are 640 and 530 K, respectively. On the other hand, the Debye temperatures of $ZnGa_2O_4:Cr^{3+}$ polycrystal estimated from the R_1- and R_2-lines are 690 and 600 K, respectively. The difference in the Debye temperature between microcrystal and polycrystal is mainly attributed to the softening of phonons in the $ZnGa_2O_4:Cr^{3+}$ microcrystal.

KEY WORDS: Transparent glass-ceramics/ Microcrystal/ $ZnGa_2O_4:Cr^{3+}$/ Optical properties/ Raman process/ Debye model/

1. INTRODUCTION

The optical properties of Cr^{3+} ion in oxide glasses have been studied extensively in the past. The ligand field strength for Cr^{3+} ion in oxide glasses is generally low, and consequently, the emission from the $^4T_2$ to $^4A_2$ is dominant even at low temperatures in most of the oxide glasses.[1-4] The transition from the $^4T_2$ to $^4A_2$ gives rise to a Stokes' shifted broad band in the red to infrared region. The emission due to the transition from the ^2E to $^4A_2$, what is called *R*-line, is barely observed at room temperature in the oxide glasses. In contrast, the *R*-line is evidently observed in Cr^{3+}-doped aluminate crystals such as spinel and ruby since high ligand field is attained in these materials.[5] Also, the emission intensity of the Stokes' shifted band as well as the *R*-line is lower in oxide glasses than in aluminate and gallate crystals.[6] Thus, from a point of view of practical application as a fluorescence material utilizing Cr^{3+} ion, oxide glasses are inferior. Nonetheless, glass is an attractive substance as an optical material because of high transparency and easiness to form any shapes. One way to obtain high emission intensity from Cr^{3+} ion in oxide glass is to introduce microcrystalline phases doped with Cr^{3+} ion into the glass.

* 田中勝久, 山口 巌, 平尾一之, 曽我直弘 : Division of Material Chemistry, Faculty of Engineering, Kyoto University, Sakyo-ku, Kyoto 606-01, Japan.

Recently, transparent glass-ceramics containing Cr^{3+}-doped microcrystals have been prepared mainly with the aim of application to a solid-state laser and a luminescence solar concentrator. The crystallization process, microstructure and optical properties of transparent glass-ceramics containing Cr^{3+}-doped aluminate and other crystals have been investigated.[7-16] The Cr^{3+} ion is effective as a photo-active center in these transparent glass-ceramics because of its high emission intensity. Besides, the Cr^{3+} ion plays a role of a nucleating agent in the precipitation process of microcrystal from the glass, as revealed from the crystallization processes of $MgAl_2O_4:Cr^{3+}$ [8] and $ZnAl_2O_4:Cr^{3+}$ [13] The latter property is advantageous for the formation of Cr^{3+}-doped microcrystals. Furthermore, the transparent glass-ceramics allow us to deduce optical properties of microcrystals, which are different than those of bulk crystals. It is known that the size of microcrystal has influence on the vibrational properties. Since many optical processes in a solid are intimately related to the vibrational properties, we can obtain information about the lattice vibration of microcrystals from optical measurements. In the present investigation, an attempt was made to prepare transparent glass-ceramics containing $ZnGa_2O_4:Cr^{3+}$ microcrystals. We report optical absorption and emission properties of transparent glass-ceramics and vibrational properties of $ZnGa_2O_4:Cr^{3+}$ microcrystals deduced from the optical measurements of the transparent glass-ceramics.

2. EXPERIMENTAL

2.1 Preparation of specimens

Glass with the composition of $6Na_2O{\cdot}18ZnO{\cdot}18Ga_2O_3{\cdot}51SiO_2{\cdot}3TiO_2{\cdot}4ZrO_2{\cdot}0.05Cr_2O_3$ (molar ratio) was prepared from reagent-grade Na_2CO_3, ZnO, Ga_2O_3, SiO_2, TiO_2, ZrO_2 and Cr_2O_3. TiO_2 and ZrO_2 were added because they were effective for lowering the temperature for melting as well as efficient as a nucleating agent.[15-17]. The raw materials were mixed thoroughly and melted in a platinum crucible at 1,600°C for 2 h in air. The melt was poured onto a stainless steel plate and quenched by being pressed with an iron plate. The resultant specimen was transparent and exhibited green color due to the Cr^{3+} ion. The amorphous state was ascertained by using X-ray diffraction analysis with CuKα radiation. The glass was heat-treated for 12 h at 680°C, which was higher by about 50°C than the glass transition temperature determined by means of the differential thermal analysis. Subsequently, the specimen was reheated at 800°C for 12 h in air. The resultant specimen was subjected to the X-ray diffraction to identify precipitated crystalline phases and to evaluate the average crystallite size. The crystallite size was estimated from the full width at half maximum (FWHM) of the X-ray diffraction peak by using the Scherrer's equation.

$ZnGa_2O_4:Cr^{3+}$ polycrystal was prepared by using the conventional solid state reaction. Reagent-grade ZnO, Ga_2O_3 and Cr_2O_3 powders were mixed thoroughly so that the composition was $ZnO{\cdot}Ga_2O_3{\cdot}0.005Cr_2O_3$ (molar ratio). The mixed powders were calcined at 1,300°C for 1 h in air. After cooled to room temperature, the specimen was pulverized. The procedure of the calcination and pulverization was repeated three times. Then, the resultant powders were cast into a pellet under a hydrostatic pressure, and sintered at 1,400°C for 3 h in air. The X-ray diffraction analysis was carried out on the sintered material in order to ascertain that the specimen was a $ZnGa_2O_4$ single phase.

2.2 Measurements of optical properties

Optical absorption spectra were measured at room temperature by using a spectrophotometer (Hitachi-330) with a Xe lamp as the light source. Emission spectra were measured at 8 to 600 K by using an Ar ion laser (Coherent Innova 70) as the excitation source. The emission was detected by using a fluorescence spectrophotometer (Hitachi-850). For the measurements below room temperature, the specimen was cooled by using a cryogenic refrigerator (Iwatani Plantech, Model CRT-006-1000) equipped with a compressor (Iwatani Plantech, Model CA101). With this apparatus, one can obtain low temperatures down to 8 K utilizing the adiabatic expansion of helium gas supplied from the compressor. For the measurements at 600 K from room temperature, the specimen was heated by using Nichrome wires; the specimen was contacted with two alumina rods around which Nichrome wires were coiled, and a current was supplied to the wires.

3. RESULTS

Figure 1 shows the X-ray diffraction patterns of the glass, transparent glass-ceramic and polycrystal specimens. All the diffraction lines in the X-ray diffraction patterns of the transparent glass-ceramics and the polycrystal are attributable to $ZnGa_2O_4$. The average crystallite size of $ZnGa_2O_4$ precipitated in the transparent glass-ceramics was estimated to be about 100 A from the FWHM of the diffraction peak corresponding to the reflection from the (440) plane. The lattice constant of the $ZnGa_2O_4$ microcrystal and polycrystal was also evaluated from the position of diffraction peaks. The results are shown in Table 1. The lattice constant of the $ZnGa_2O_4$ microcrystal is almost identical with that of the $ZnGa_2O_4$ polycrystal.

Optical absorption spectra of the glass and transparent glass-ceramics are shown in Fig. 2. According to the Tanabe-Sugano diagram, the absorption bands at around 15,900 cm^{-1} and

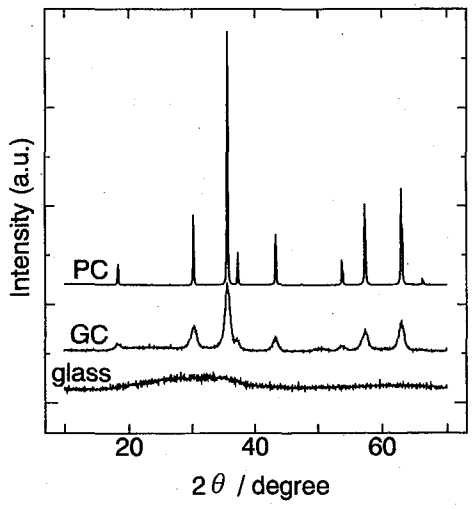

Fig. 1. X-ray diffraction patterns of glass, transparent glass-ceramics (denoted by GC in the figure) and polycrystal (denoted by PC in the figure). All the diffraction lines in the X-ray diffraction patterns of the transparent glass-ceramics and polycrystal are attributable to $ZnGa_2O_4$.

Table 1. Average crystallite size and lattice constant of $ZnGa_2O_4:Cr^{3+}$ microcrystal precipitated in the transparent glass-ceramics and $ZnGa_2O_4:Cr^{3+}$ polycrystal.

	Crystallite size (A)	Lattice constant (A)
$ZnGa_2O_4:Cr^{3+}$		
Microcrystal	100	8.344
Polycrystal	—	8.346

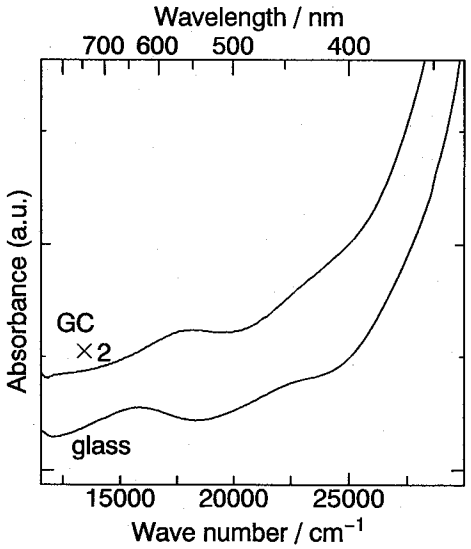

Fig. 2. Optical absorption spectra of glass and transparent glass-ceramics measured at room temperature. The assignments of the absorption peaks are presented in the text.

23,500 cm^{-1} observed for the glass correspond to the $^4A_2-^4T_2$ and $^4A_2-^4T_1$ transitions, respectively. Similarly, the absorption bands at around 16,300 cm^{-1} and 22,500 cm^{-1} in the spectrum of the transparent glass-ceramics are assigned to the $^4A_2-^4T_2$ and $^4A_2-^4T_1$ transitions, respectively. When the absorption peak positions are represented by ν_1 and ν_2 where ν_1 and ν_2 respectively correspond to the $^4A_2-^4T_2$ and $^4A_2-^4T_1$ transitions, following equations hold:[18]

$$\nu_1 = 10Dq, \tag{1a}$$

$$\nu_2 = 7.5B + 15Dq - \frac{1}{2}(225B^2 + 100Dq^2 - 180BDq)^{1/2}, \tag{1b}$$

Table 2. Ligand field strength, Dq, and Racah parameter, B, for the Cr^{3+} ion in the $6Na_2O{\cdot}18ZnO{\cdot}18Ga_2O_3{\cdot}51SiO_2{\cdot}3TiO_2{\cdot}4ZrO_2{\cdot}0.05Cr_2O_3$ glass and $ZnGa_2O_4:Cr^{3+}$ microcrystal precipitated from the glass.

	Dq (cm^{-1})	B (cm^{-1})	Dq/B
Glass	1,590	827	1.9
$ZnGa_2O_4:Cr^{3+}$ microcrystal	1,630	610	2.7

where Dq is the ligand field strength and B is the Racah parameter. By using Eqs. (1a) and (1b), we evaluated the values of Dq and B for the glass and transparent glass-ceramics. The results are shown in Table 2.

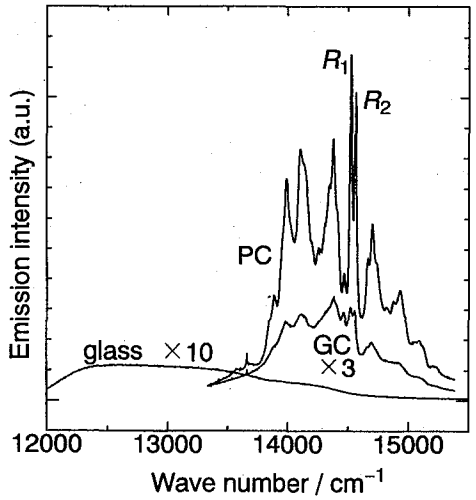

Fig. 3. Emission spectra of glass, transparent glass-ceramics, and $ZnGa_2O_4$: Cr^{3+} polycrystal measured at room temperature. The excitation was carried out by using an Ar ion laser (all lines).

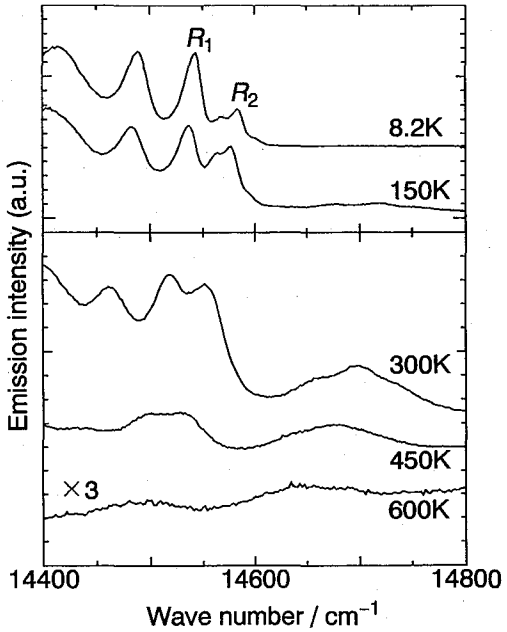

Fig. 4. Temperature variation of emission spectrum of $ZnGa_2O_4:Cr^{3+}$ microcrystal precipitated in the transparent glass-ceramics. It should be noted that the scale of the abscissa for the top two spectra is different than that for the bottom three spectra.

In Fig. 3 are shown the emission spectra of glass, transparent glass-ceramics, and $ZnGa_2O_4:Cr^{3+}$ polycrystal measured at room temperature. The glass manifests a broad and weak Stokes' shifted band at around 13,000 cm^{-1}. In contrast, intense peaks with narrow linewidth are observed at around 14,500 and 14,550 cm^{-1} in the spectrum of the $ZnGa_2O_4:Cr^{3+}$ polycrystal. These peaks are R_1- and R_2-lines, respectively. These lines also appear in the spectrum of the transparent glass-ceramics, although the intensity is lower compared with the spectrum of the polycrystal. The emission bands at around 13,900, 14,000, 14,100 and 14,400 cm^{-1}, which are observed for both transparent glass-ceramics and polycrystal, are assigned to the vibronic sidebands of the transition from the ^2E to $^4A_2$ levels. The emission bands observed in the region higher than 14,600 cm^{-1} are ascribed to the hot bands.[5] Figure 4 shows the temperature variation of emission spectrum for $ZnGa_2O_4:Cr^{3+}$ microcrystal precipitated in the transparent glass-ceramics. In this figure, the scales of the abscissa for the top two spectra are different than those for the bottom three spectra. The R_1- and R_2-lines manifest broad linewidth and low intensity in the spectra above room temperature. In particular, the R-lines are barely observed in the spectra above 450 K. Figure 5 shows the temperature dependence of emission spectrum of $ZnGa_2O_4:Cr^{3+}$ polycrystal. The temperature variations of R-lines are similar to those for the $ZnGa_2O_4:Cr^{3+}$ microcrystal; the linewidth of the R-lines increases and the intensity of those lines decreases with an increase in temperature.

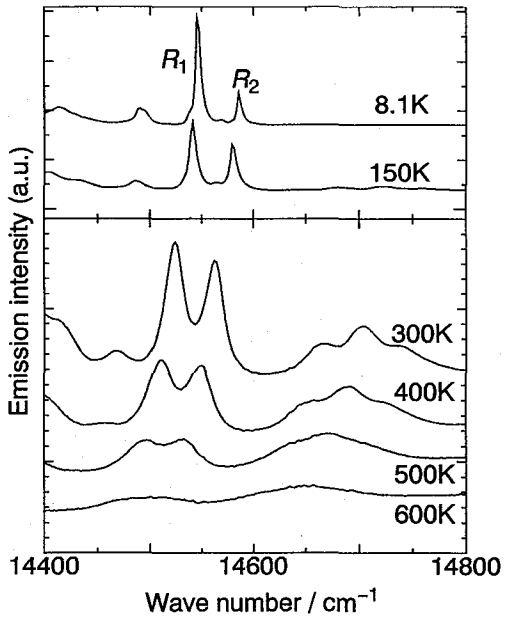

Fig. 5. Temperature variation of emission spectrum of $ZnGa_2O_4:Cr^{3+}$ polycrystal. The scale of the abscissa for the top two spectra is different than that for the bottom four spectra.

4. DISCUSSION

As shown in Table 2, the ligand field strength Dq is larger for the transparent glass-ceramics than for the glass. This fact indicates that Cr^{3+} ions are incorporated in the $ZnGa_2O_4$

microcrystalline phases in the transparent glass-ceramics and the $ZnGa_2O_4$ microcrystal offers higher ligand field to the Cr^{3+} ion than the glass. The B value is smaller for the transparent glass-ceramics than for the glass, indicating that the interaction between the $3d$ orbitals of Cr^{3+} ion and the $2p$ orbitals of oxide ions is larger in the $ZnGa_2O_4:Cr^{3+}$ microcrystal than in the glass. Presumably, the interionic separation between Cr^{3+} and O^{2-} is shorter in the $ZnGa_2O_4:Cr^{3+}$ microcrystal than in the glass, leading to the higher ligand field strength and smaller B value for the $ZnGa_2O_4:Cr^{3+}$ microcrystal. The high ligand field strength in $ZnGa_2O_4$ is also reflected in the emission spectra. As shown in Fig. 3, the emission bands which correspond to the transition from the ^2E to $^4A_2$ are clearly observed for the $ZnGa_2O_4:Cr^{3+}$ microcrystal while the emission spectrum of the glass consists of only broad Stokes' shifted band due to the $^4T_2-{}^4A_2$ transition.

It is known that the peak position of zero-phonon line changes with temperature. In Raman process, the temperature dependence of peak position of zero-phonon line is expressed by the following equation when the Debye model is assumed for the vibrational density of state :[19]

$$\varepsilon(T)=\varepsilon(0)+\alpha\left(\frac{T}{\theta_D}\right)^4\int_0^{\theta_D/T}\frac{x^3}{e^x-1}dx. \tag{2a}$$

Here α is given by

$$\alpha=\frac{3h\omega_D{}^4}{4\pi^3\rho v^5}\left[\langle i\,|\,V^{(2)}\,|\,i\rangle+\sum_{m\neq i}\frac{|\,\langle i\,|\,V^{(1)}\,|\,m\rangle\,|^2}{W_i-W_m}\right], \tag{2b}$$

where h is the Planck constant, ω_D is the cut-off frequency in the Debye model, ρ is the density, v

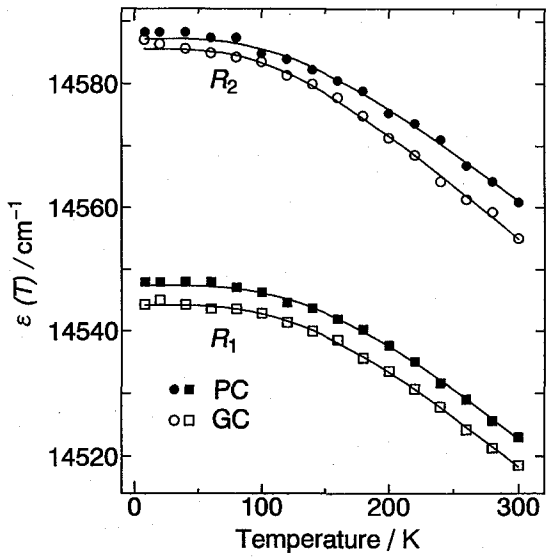

Fig. 6. Temperature dependence of peak position of R_1- and R_2-lines for $ZnGa_2O_4:Cr^{3+}$ microcrystal precipitated in the transparent glass-ceramics and for the $ZnGa_2O_4:Cr^{3+}$ polycrystal. The open and closed symbols correspond to the $ZnGa_2O_4:Cr^{3+}$ microcrystal and polycrystal, respectively. R_1 and R_2 denote the R_1- and R_2-lines, respectively. The solid curves are drawn by assuming the Raman process for the electronic transition and the Debye model for the vibrational density of state (Eqs. (2a) and (2b)).

is the sound velocity, $V^{(1)}$ and $V^{(2)}$ are relevant to the local strain field, and W_i and W_m are the energy levels of i-th and m-th states, respectively. In Fig. 6 are shown the temperature variations of peak positions of R_1- and R_2-lines for the $ZnGa_2O_4:Cr^{3+}$ microcrystal precipitated in the transparent glass-ceramics and for the $ZnGa_2O_4:Cr^{3+}$ polycrystal. The open and closed symbols represent the experimental data for the $ZnGa_2O_4:Cr^{3+}$ microcrystal and $ZnGa_2O_4:Cr^{3+}$ polycrystal, respectively. The solid curves are calculated ones, which were fitted to the experimental data by using Eqs. (2a) and (2b) with parameters $\varepsilon(0)$, α and θ_D given in Table 3. Only the experimental data obtained below room temperature were adopted in the calculation, because it was difficult to determine the accurate peak positions of linewidth of R_1- and R_2-lines in the emission spectra above room temperature owing to the broadness and weakness of intensity. Table 3 indicates that the Debye temperature obtained from the temperature dependence of the R_1-line is not identical with the Debye temperature derived from the R_2-line. The reason for this incompatibility is unclear, but the properties of phonons relevant to the electronic transitions corresponding to R_1- and R_2-lines may be different from each other. In this sense, the Debye temperatures obtained from the present optical measurements are inevitably different than those derived from the other properties such as specific heat, Debye-Waller factor, and recoil-free fraction. Table 3 also shows that the Debye temperature for the $ZnGa_2O_4:Cr^{3+}$ microcrystal is lower than that for the $ZnGa_2O_4:Cr^{3+}$ polycrystal. As well known, there is a general tendency that the Debye temperature decreases with a decrease in the size of crystal because of the softening of phonons on the surface of the microcrystal.[20,21] For instance, it was reported that the Debye temperature of microcrystalline Au of 60 A is 134 K while that of bulk Au is 168 K.[20] In the present case, we speculate that the lower Debye temperature of the $ZnGa_2O_4:Cr^{3+}$ microcrystal compared with the polycrystal is mainly attributed to the softening of lattice vibration at the interface between microcrystal and glass matrix. As for the Au microcrystal, in contrast with the dependence of the Debye temperature on the size of crystal, the lattice constant is independent of the size of the crystal.[20] A similar result was obtained for the present $ZnGa_2O_4:Cr^{3+}$ microcrystal, as indicated in Table 1; the lattice constant of the $ZnGa_2O_4:Cr^{3+}$ microcrystal is almost identical to that of polycrystal.

It is found from Figs. 3 to 5 that the intensity of the R_1- and R_2-lines is lower and the linewidth of these lines is broader for the $ZnGa_2O_4:Cr^{3+}$ microcrystal than for the polycrystal. The broad linewidth for the $ZnGa_2O_4:Cr^{3+}$ microcrystal implies the site-to-site distribution of Cr^{3+} ions in this material. The wide distribution of Cr^{3+} ion sites arises from possible

Table 3. Peak position of R_1- and R_2-lines at 0 K, $\varepsilon(0)$, the parameter α in Eqs. 2a and 2b, and Debye temperature, θ_D, for $ZnGa_2O_4:Cr^{3+}$ microcrystal precipitated in the transparent glass-ceramics and $ZnGa_2O_4:Cr^{3+}$ polycrystal.

	$\varepsilon(0)$ (cm^{-1})	α (cm^{-1})	θ_D (K)
R_1-line			
$ZnGa_2O_4:Cr^{3+}$ microcrystal	14,544	−410	640
$ZnGa_2O_4:Cr^{3+}$ polycrystal	14,547	−450	690
R_2-line			
$ZnGa_2O_4:Cr^{3+}$ microcrystal	14,586	−340	530
$ZnGa_2O_4:Cr^{3+}$ polycrystal	14,587	−350	600

incorporation of Ti and Zr into the $ZnGa_2O_4:Cr^{3+}$ microcrystalline phase as well as the existence of Cr^{3+} ions on the surface region of the microcrystal. The lower intensity for the $ZnGa_2O_4:Cr^{3+}$ microcrystal may reflect lower ligand field strength compared with the $ZnGa_2O_4:Cr^{3+}$ polycrystal.

5. CONCLUSION

Transparent glass-ceramics containing $ZnGa_2O_4:Cr^{3+}$ microcrystals were successfully prepared by the heat treatment of $6Na_2O{\cdot}18ZnO{\cdot}18Ga_2O_3{\cdot}51SiO_2{\cdot}3TiO_2{\cdot}4ZrO_2{\cdot}0.05Cr_2O_3$ (molar ratio) glass. Incorporation of Cr^{3+} ions into the $ZnGa_2O_4$ microcrystalline phase was demonstrated from the optical absorption and emission spectra. As revealed from the full width at half maximum of X-ray diffraction peak, the average crystallite size of $ZnGa_2O_4:Cr^{3+}$ is about 100 A. The ligand field strength around the Cr^{3+} ion is higher in the $ZnGa_2O_4:Cr^{3+}$ microcrystal than in the glass, resulting in the appearance of *R*-lines in the emission spectrum of the transparent glass-ceramics. The temperature dependence of peak position of the R_1- and R_2-lines for the transparent glass-ceramics and $ZnGa_2O_4:Cr^{3+}$ polycrystal is describable in terms of the Raman process assuming the Debye model for the vibrational density of state. The Debye temperature of the $ZnGa_2O_4:Cr^{3+}$ microcrystal is lower than that of the $ZnGa_2O_4:Cr^{3+}$ polycrystal, indicating that the softening of phonons takes place in the $ZnGa_2O_4:Cr^{3+}$ microcrystal.

6. ACKNOWLEDGEMENT

This work was financially supported by a Grant-in-Aid for Encouragement of Young Scientists (No. 05750747).

REFERENCES

(1) A. van Die, A.C.H.I. Leenaers, G. Blasse and W.F. van der Weg, *J. Non-Cryst. Solids,* **99**, 32 (1988).
(2) L.J. Andrews, A. Lempicki and B.C. McCollum, *J. Chem. Phys.,* **74**, 5526 (1981).
(3) F. Rasheed, K.P. O'Donnell, B. Henderson and D.B. Hollis, *J. Phys.: Condens. Matter,* **3**, 1915 (1991).
(4) F. Rasheed, K.P. O'Donnell, B. Henderson and D.B. Hollis, *J. Phys.: Condens. Matter,* **3** , 3825 (1991).
(5) D.L. Wood, G.F. Imbusch, R.M. Macfarlane, P. Kisliuk and D.M. Larkin, *J. Chem. Phys.,* **48**, 5255 (1968).
(6) T. Izumitani, X. Zou and Y. Wang, The Physics of Non-Crystalline Solids, ed. by L.D. Pye, W.C. LaCourse and H.J. Stevens, Taylor & Francis, London, p. 603 (1992).
(7) R. Reisfeld and C.K. Jørgensen, Structure and Bonding, 49, Springer-Verlag, Berlin Heidelberg, p. 1 (1982).
(8) F. Durville, B. Champagnon, E. Duval, G. Boulon, F. Gaume, A.F. Wright and A.N. Fitch, *Phys. Chem. Glasses,* **25**, 126 (1984).
(9) F. Durville, B. Champagnon, E. Duval and G. Boulon, *J. Phys. Chem. Solids,* **46**, 701 (1985).
(10) R. Reisfeld, A. Kisilev, A. Buch and M. Ish-Shalom, *J. Non-Cryst. Solids,* **91**, 333 (1987).
(11) A. Kisilev, R. Reisfeld, A. Buch and M. Ish-Shalom, *Chem. Phys. Lett.,* **129**, 450 (1986).
(12) H. Liu, R. Knutson and W.M. Yen, *Phys. Rev.,* **B41**, 8 (1990).
(13) W. Nie, G. Boulon, C. Mai, C. Esnouf, R. Xu and J. Zarzycki, *J. Non-Cryst. Solids,* **121**, 282 (1990).
(14) X.F. Liu, J.M. Parker, E.A. Harris and C. Topacli, The Physics of Non-Crystalline Solids, ed. by L.D. Pye, W.C. LaCourse and H.J. Stevens, Taylor & Francis, London, p. 642 (1992).
(15) K. Tanaka, K. Hirao, T. Ishihara and N. Soga, *J. Ceram. Soc. Jpn.,* **101**, 102 (1993).
(16) T. Ishihara, K. Tanaka, K. Hirao and N. Soga, *J. Soc. Mater. Sci. Jpn.,* **42**, 484 (1993).
(17) K. Tanaka, T. Mukai, T. Ishihara, K. Hirao, N. Soga, S. Sogo, M. Ashida and R. Kato, *J. Am. Ceram.*

Soc., **76**, 2839 (1993).
(18) J.E. Huheey, E.A. Keiter and R.L. Keiter, Inorganic Chemistry, Fourth Edition, HarperCollins College Publisher, New York, Chap. 11 (1993).
(19) D.E. McCumber and M.D. Sturge, *J. Appl. Phys.* **34**, 1682 (1963).
(20) J. Harada and K. Ohshima, *Surf. Sci.* **106**, 51 (1981).
(21) Y. Kashiwase, I. Nishida, Y. Kainuma and K. Kimoto, *J. Phys. Soc. Jpn.* **38**, 899 (1975).